CONFIDENTIAL

NACA

RESEARCH MEMORANDUM

PRELIMINARY INVESTIGATION OF POROUS WALLS AS A MEANS OF REDUCING TUNNEL BOUNDARY EFFECTS AT LOW-SUPERSONIC MACH NUMBERS

By William J. Nelson and Frederick Bloetscher

Langley Aeronautical Laboratory
Langley Air Force Base, Va.

NATIONAL ADVISORY COMMITTEE
FOR AERONAUTICS

WASHINGTON

September 13, 1950

CONFIDENTIAL

Classification cancelled (or changed to Unclassified)

By Authority of NSA Technical Journal Announcement #62

(OFFICER AUTHORIZED TO CHANGE)

By... E. Mayfield

.....
GRADE

.....11 APR 61
DATE

NATIONAL ADVISORY COMMITTEE FOR AERONAUTICS

RESEARCH MEMORANDUM

PRELIMINARY INVESTIGATION OF POROUS WALLS AS A MEANS OF REDUCING TUNNEL BOUNDARY EFFECTS AT LOW-SUPERSONIC MACH NUMBERS

By William J. Nelson and Frederick Bloetscher

SUMMARY

The use of porous-walled tunnels at supersonic Mach numbers as a means of avoiding reflection of a stream disturbance extending to the walls is discussed. Calculated shock-reflection characteristics of porous materials are presented in the form of design charts for Mach numbers up to 1.5 and incident shock deviations up to 6°. The charts presented indicate that for walls of a given porosity there exists a range of incident shocks representing certain combinations of stream deviation and Mach number for which no reflected disturbance will occur; for all other incident shocks, reflections occur but the stream deviation across the reflected disturbance is less than that for a solid boundary. Results obtained in experiments in which the bow shock from a 4° wedge at a Mach number of 1.2 was reflected from sintered-bronze and bonded-screen walls are consistent with the calculated characteristics.

INTRODUCTION

The development of wind tunnels in which the free-air characteristics of bodies might be obtained through the transonic-speed range has received the attention of many investigators both in this country and abroad. Air streams have been generated throughout the transonic regime in tunnels of constant geometry by the withdrawal of air through slotted or porous walls (references 1 to 5). The alleviation of tunnel choking has also been effected by the use of longitudinally slotted walls through the test section (references 3, 4, and 6). At subsonic and low-transonic airspeeds, pressures measured on nonlifting bodies of revolution in the slotted tunnels are in reasonable agreement over most of the body with those measured on bodies of the same size in much larger closed tunnels. It was indicated in reference 4 that pressure differences encountered over the forward part of the body at Mach numbers

greater than 1.08 were to a large extent caused by reflection of the model bow wave from the tunnel boundary. Efforts to minimize the magnitude of the reflected disturbances from slotted walls are in progress as part of the NACA transonic-tunnel program. This program also includes the investigation of the disturbances reflected from materials of uniform porosity. Prior experimentation in this field was carried out by George P. Wood of the Langley Laboratory who established by means of interferograms that marked reductions in the intensity of reflected disturbances could be effected by the use of porous boundaries.

The purpose of the present investigation was to determine the shock-reflection characteristics of porous jet boundaries at low-supersonic Mach numbers. An analysis has been made to determine the strength and sign of disturbances caused by the reflection of two-dimensional compression shocks of the weak family from boundaries of uniform porosity. The results of these calculations, which were terminated arbitrarily at a Mach number of 1.5 and an initial stream deviation of 6°, are presented as a series of charts for several values of porosity. The application of the charts to the determination of the shock-reflection characteristics of any materials of known porosity is discussed. A comparison of calculated and experimental disturbances reflected from readily available sintered-bronze and bonded-screen walls is also presented. These tests were conducted in a $2\frac{1}{4}$ by $4\frac{1}{2}$-inch jet in which initial stream deviations of approximately 2° were produced with a sting-supported wedge mounted parallel to the porous walls. This work was completed in November 1949 at the Langley Internal Aerodynamics Section.

SYMBOLS

a	sonic velocity, feet per second
g	acceleration due to gravity, feet per second per second
M	Mach number
p	local pressure, pounds per square foot
Δp	pressure behind reflected wave minus free-stream static pressure, pounds per square foot
T	temperature, °F absolute
V	velocity component normal to porous wall, feet per second
δ	angular change in direction of flow; positive value indicates compression, negative value indicates expansion, degrees

ρ mass density, slugs per cubic foot

Subscripts:

i incident disturbance

r reflected disturbance

0 stagnation conditions

1 free-stream conditions

2 conditions following incident wave

3 conditions following reflected wave

ANALYSIS

In supersonic streams, changes in direction of flow are propagated along shock or characteristic Mach lines. These disturbances, if they reach the stream boundary, give rise to reflected disturbances, the nature of which are determined by the boundary conditions. At a solid wall the physical requirement that the flow possess no component normal to the wall in general results in a reflected disturbance, across which the stream deviation is equal to that across the incident disturbance; thus, as shown in figure 1, a shock wave is reflected as a shock. At an open boundary, equality of static pressure along the edge of the stream can be preserved only by the reflection of compression disturbances as expansions. Since expansions are propagated along a region lying entirely behind the Mach line, whereas shock fronts reach ahead of the Mach line, it is apparent that interference effects resulting from the reflection of bow shocks will reach farther upstream in a tunnel with a closed boundary than in the open jet tunnel of equal size. The opposite is true if the initial disturbance reaching the wall is an expansion; this case, however, is encountered in transonic research much less frequently than that where the initial disturbance is the bow shock.

The fact that the reflected waves from the solid tunnel and the open jet are of opposite sign suggests the possibility of avoiding reflected disturbances through the use of a porous surface which, imposing neither the solid-boundary requirement of parallel flow nor the open-jet requirement of equality of static pressure along the boundary, would permit that part of the stream directed toward the boundary to pass outward without disturbing the pressure field behind the incident disturbance (fig. 1). To evaluate the porosity requirements of

such a boundary, the flow rate normal to the undisturbed stream, together with the pressure change corresponding to two-dimensional changes in direction of flow, has been calculated by the methods of references 7 and 8. These parameters, expressed nondimensionally in terms of the stream stagnation conditions, are presented as a function of the angular deflection of the stream for several Mach numbers below 1.5 in figure 2. The rate of air flow through the wall and the pressure difference available for effecting this flow can be determined directly from these curves and the stream stagnation conditions if it is assumed that: (1) the porous wall is parallel to the undisturbed stream, (2) the pressure difference across the porous wall is zero ahead of the incident disturbance, and (3) the flow of air behind the incident disturbance is out of the tunnel. The first assumption is readily satisfied by maintaining constant tunnel cross section through the test region, and the second, by establishing uniform velocity ahead of the incident disturbance. The third assumption restricts the calculations to the case of incident shock disturbances, but, in general, this restriction represents no serious limitation since the model length will usually be determined by the bow shock and its reflection.

The nondimensional normal flow rates and pressure differences from figure 2 are plotted as a single parameter $\frac{\rho_2 V_2/\rho_0 a_0}{\Delta(p/p_0)}$ in figure 3. Because of the variation in this parameter with both Mach number and angular change in stream direction, it appears improbable that reflections will be avoided with a single material over any very wide range of disturbances. The shock curves are based on discrete compressions and are therefore strictly applicable only where the turning is accomplished through a single oblique shock. The expansion curves, however, are based upon isentropic flow, and since expansion at supersonic Mach numbers occurs continuously across a band of finite width, the porosity required to avoid reflections of a single disturbance is not constant but varies continuously from that corresponding to zero turning to the final deviation.

Because no one wall will produce complete freedom from reflection for all incident disturbances and since a reduction of the deviation across reflected disturbances may in many cases prove advantageous, it is desirable to determine the change in flow direction across disturbances reflected from walls of known porosity. To facilitate the determination of the stream deviation across reflected disturbances, a series of charts for constant values of $\rho g V/\Delta p$ has been prepared (fig. 4). The selected ratios of weight-flow rate to pressure drop $\left(\frac{\rho g V}{\Delta p} = 0.0055, 0.011, 0.018, \text{and } 0.024\right)$ cover the range of general interest in transonic-tunnel applications. The static pressure ahead of the incident disturbance was assumed constant at a value equal to 2116 pounds

per square foot; the assumed stagnation temperature was 520° F absolute. The determination of the change in direction of flow across the reflected disturbance was accomplished by a step process, in which the weight-flow rate normal to the surface for assumed values of δ_r was calculated and then the value which satisfied the relation $\frac{\rho g V}{\Delta p} \Delta p = \rho_3 g M_3 a_3 \sin(\delta_i - \delta_r)$ was determined graphically.

At the lowest porosity for which the calculations were made $\left(\frac{\rho g V}{\Delta p} = 0.0055\right)$, the reflected disturbance and the incident disturbance are of the same sign; the angular deviation of the stream, however, is smaller across the reflected disturbance and varies from one-half the incident deflection at low Mach numbers to two-thirds δ_i as the value of M approached 1.5. The boundary line along which these curves are terminated corresponds to the maximum total angle through which the flow can be turned by weak shocks, incident and reflected.

Because the flow deviation across the disturbance reflected from a porous wall is appreciably less than that across the corresponding solid-wall reflection, the disturbance reflected from the porous-walled tunnel will lie behind the corresponding solid-wall reflection; thus, the length of model ahead of the reflected disturbance is increased by the use of porous walls. The pressure change also is smaller across the disturbance reflected from the porous wall; therefore, its effect on the aerodynamic characteristics of a body extending through the reflected disturbance would be appreciably reduced and may in many cases be of negligible importance. This latter characteristic of disturbances reflected from porous walls is of special significance at low-supersonic speeds where disturbances propagate at very large angles to the flow, and termination of the model ahead of the reflected disturbance is not practical.

Increasing the wall porosity reduces the change in angle across the reflected waves and the sign of the disturbance is first reversed at the low Mach numbers and small values of the incident stream deflection. (Compare figs. 4(b), 4(c), and 4(d) with fig. 4(a).) Between the regions where incident shocks are reflected with the same sign and where the sign of the reflected disturbance is reversed, there exists a limited range of combinations of M and δ_i for which incident shocks are not reflected. Note also that the range of regular reflections increases with porosity until the point is reached where the reflection occurs as an expansion; from this point on the boundary corresponds to the maximum deflection which can be taken through the incident shock. For other values of porosity $\rho g V/\Delta p$ the stream deviation across the reflection of a given incident shock may be obtained readily by interpolation. If, however, the weight-flow rate through the new surface varies nonlinearly with the pressure difference, a second or third approximation may be necessary.

Charts similar to those of figure 4 have been prepared for two samples of readily obtained porous materials (fig. 5). The porosity characteristics of these materials (fig. 6) differed markedly from the linear relationship between flow rate and pressure drop assumed previously. It appears from the curves presented that, in any practical application of porous walls to reduce shock reflections, the porosity will be determined by a compromise based upon the anticipated operating range of the tunnel. Thus, of the two materials whose characteristics are presented in figure 5, the disturbance reflected from the bonded-screen wall will be farther downstream than that reflected from the porous bronze except for a small region at low Mach numbers and small deviations where the fronts of the reflected disturbances for both cases coincide since the forward edge of the expansion coincides with the Mach line. For those conditions at which the incident shock reflects as an expansion, the leading edge of the reflected disturbance in the porous-walled tunnel is equal to that in the open jet. The deviation across the reflected expansion, however, is smaller in the porous tunnel.

EXPERIMENT

To corroborate the preceding analysis, the reflections of incident shocks from both the sintered-bronze and bonded-screen walls obtained from schlieren photographs are compared with the calculated reflections read from figure 5.

Apparatus and Tests

The general arrangement of the experimental equipment used is shown in the photograph of figure 7(a). The wedge shown in the tunnel was used to initiate the stream disturbance in the original tests. Air at elevated pressure and temperature was accelerated to sonic velocity through a 70:1 contraction ahead of the $2\frac{1}{4}$- by $4\frac{1}{2}$-inch rectangular tunnel. The supersonic region was developed by removal of air through porous walls (reference 2). The side walls of the tunnel were formed by glass plates; the upper and lower walls were porous. Two sets of porous walls were used in the investigation: a relatively high density sintered bronze and a low-density screen sandwich. These materials were selected solely because of their availability; their characteristics are discussed previously in this paper. For the specimens used, the porosity through the test region varied less than 5 percent from the mean.

The wedge used to generate the initial disturbance in these tests is shown in detail in figure 7(b). The total angle of wedge was 4°; to reduce boundary-layer interference effects along the side walls, the wedge was terminated 1/4 inch from the glass plates. Steel strips 0.010 inch thick extended to the window to eliminate flow across the wing tip; these strips were found to be unnecessary and were removed for the tests with the screen floors since disturbances created by them obscured the reflected wave in the schlieren photograph.

The schlieren optical system used in recording the flow field along the tunnel walls employed front-surfaced mirrors 6 inches in diameter with a focal length of 48 inches. The light source was a high intensity spark of approximately 10 microseconds' duration.

Stagnation pressure and temperature were recorded at a point well ahead of the converging section at the entrance to the porous section.

Results and Discussion

Typical schlieren photographs of the flow about a 4° wedge mounted in the experimental tunnel with porous walls are presented in figure 8. The many fine lines observed in the schlieren photographs are caused by the surface roughness of the porous walls. The slope of these fine lines was measured to determine the Mach number on both sides of the incident and reflected disturbances. From the change in Mach number across the disturbance, the flow deviation was determined by using two-dimensional theory. The results of these measurements are shown in figure 5 for several tests at Mach numbers close to 1.20; differences between the experimental and calculated values of δ_r are within the experimental accuracy.

Rows of white dots on the schlieren photographs (fig. 8) mark the incident shock and the position of the reflected disturbance as determined from two-dimensional theory by using the measured values of M_1 and M_2 and the calculated value of δ_r from figure 5. Variations in the flow deviation across the incident shocks result from inaccuracies in alinement of the wedge, the leading-edge radius (0.0007 in.) which causes detachment of the bow shock, and experimental difficulties in determining Mach number precisely from schlieren photographs. The calculations indicate that 1.8° and 2.1° incident shocks at $M \approx 1.2$ will reflect as weak shocks, $\delta_r = 0.6$ and 0.8, respectively, from the sintered-bronze walls and as expansions from the bonded-screen walls. From the schlieren photographs, however, the reflected disturbances appear as regions of expansion followed by a region of continuous compression; this result is most obvious in the reflection from the bonded-screen walls. This overexpansion is attributed to an effective increase in porosity at the point of intersection of the incident shock and the wall where, because of wall depth, air entering the floor immediately

behind the shock can flow forward within the wall as well as vertically through it. Thus, the rate at which air enters the wall is greater than can be maintained at equilibrium downstream and the subsequent reduction of the flow rate to equilibrium is accomplished through the compression, turning the air back into the jet. This effect is greatest in the case of the bonded-screen walls because of their greater depth, 0.25 inch as opposed to 0.080 inch for the sintered bronze. Since the calculations make no allowance for this effect, local variations in slope of the calculated and observed reflected disturbance are not surprising. Downstream of the local overexpansion, the slope of the many fine lines through the flow is consistent with that calculated from the mean calibration curve for the entire floor.

CONCLUSIONS

From the preliminary investigation of the reflection of two-dimensional bow shocks from porous surfaces, the following conclusions are drawn:

From analysis:

1. Reflection of model leading-edge shocks reaching a tunnel wall can be avoided by the use of porous walls. The required wall porosity for complete cancellation of incident disturbances varies with intensity of disturbance and is therefore a function of both the deviation across the initial disturbance and tunnel Mach number.

2. For all disturbances other than that corresponding to complete cancellation, the stream deviation across the reflected disturbance is less than that from either a solid or open boundary.

3. In general, the length of model over which free-air flow conditions may be represented in a wind tunnel is greater for a porous-walled tunnel than for solid-boundary tunnels.

From experiments with a 4° wedge at a Mach number of 1.2:

1. The flow deviation across reflected disturbances is consistent with the calculations.

2. Wall thickness produces an effective increase in porosity at points of pressure discontinuity; thus shock reflections tend to occur as expansions with subsequent compression back to equilibrium conditions.

Langley Aeronautical Laboratory
National Advisory Committee for Aeronautics
Langley Air Force Base, Va.

REFERENCES

1. Nelson, William J., and Bloetscher, Frederick: Preliminary Investigation of a Variable Mach Number Two-Dimensional Supersonic Tunnel of Fixed Geometry. NACA RM L9D29a, 1949.

2. Nelson, William J., and Klevatt, Paul L.: Preliminary Investigation of Constant-Geometry, Variable Mach Number, Supersonic Tunnel with Porous Walls. NACA RM L50B01, 1950.

3. Wright, Ray H., and Ward, Vernon G.: NACA Transonic Wind-Tunnel Test Sections. NACA RM L8J06, 1948.

4. Ward, Vernon G., Whitcomb, Charles F., and Pearson, Merwin D.: An NACA Transonic Test Section with Tapered Slots Tested at Mach Numbers to 1.26. NACA RM L50B14, 1950.

5. Bates, George P.: Preliminary Investigation of 3-Inch Slotted Transonic Wind-Tunnel Test Sections. NACA RM L9D18, 1949.

6. Scroggs, A. M.: Data Report - Boeing Wind Tunnel Test No. 115 - Test No. 1 of the Slotted Test Sections in the $\frac{1}{20}$-Scale Model Wind Tunnel. Document No. D-9400, Boeing Airplane Co., Jan. 27, 1949.

7. Burcher, Marie A.: Compressible Flow Tables for Air. NACA TN 1592, 1948.

8. Neice, Mary M.: Tables and Charts of Flow Parameters across Oblique Shocks. NACA TN 1673, 1948.

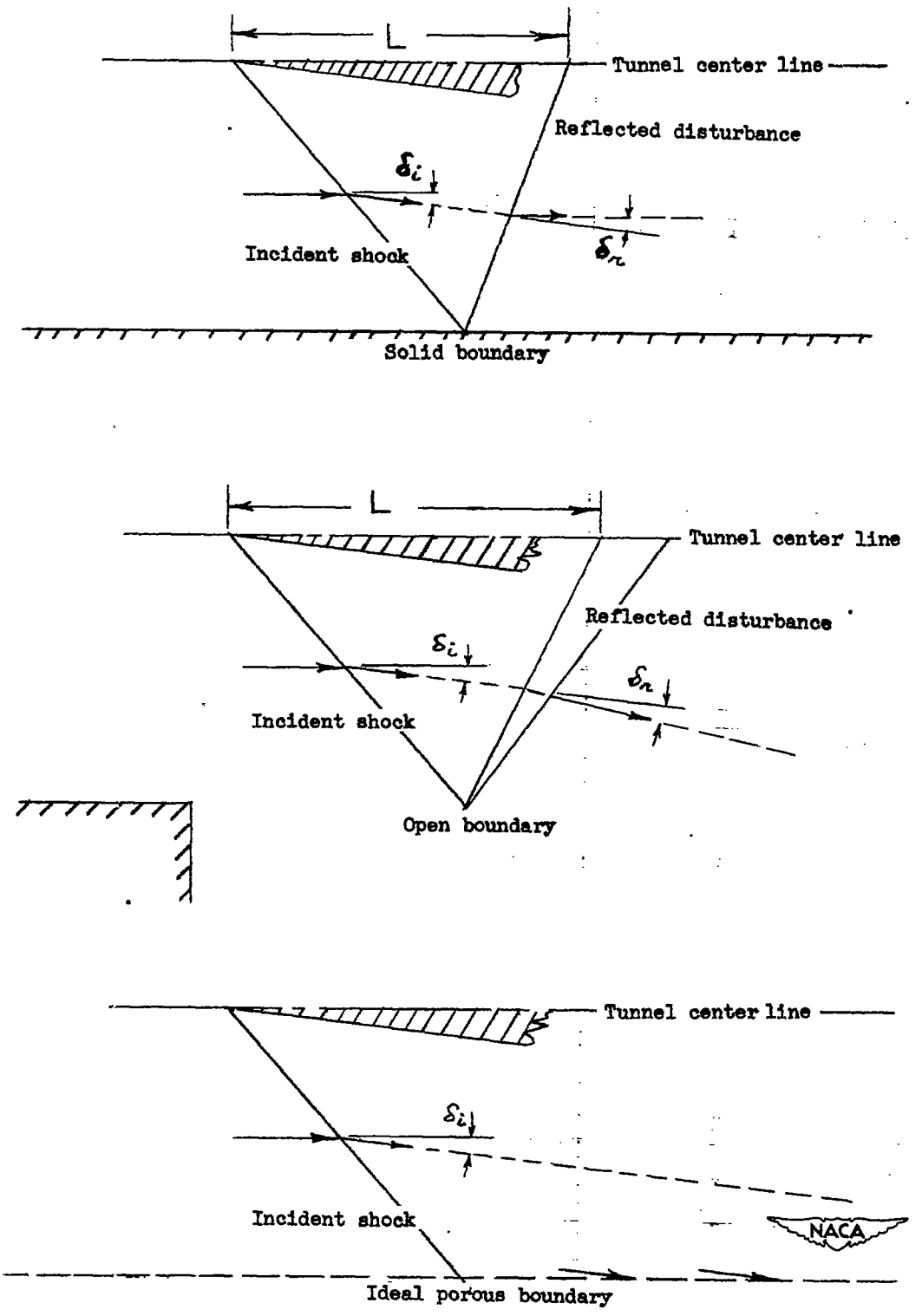

Figure 1.- Schematic diagram of shock reflection from solid, open, and porous tunnel boundaries.

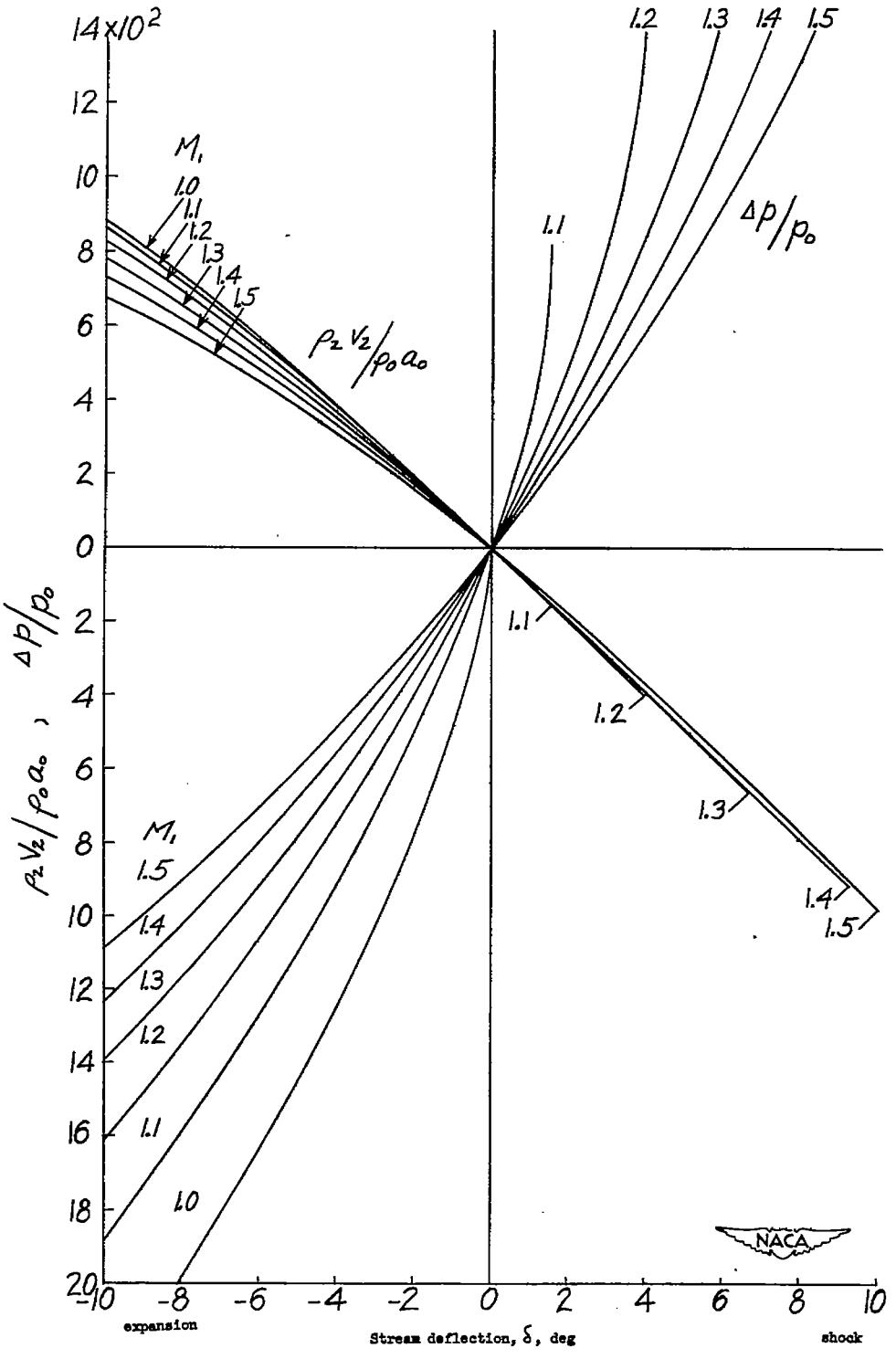

Figure 2.- Effect of stream disturbance on mass-flow component normal to the tunnel axis and on the stream pressure.

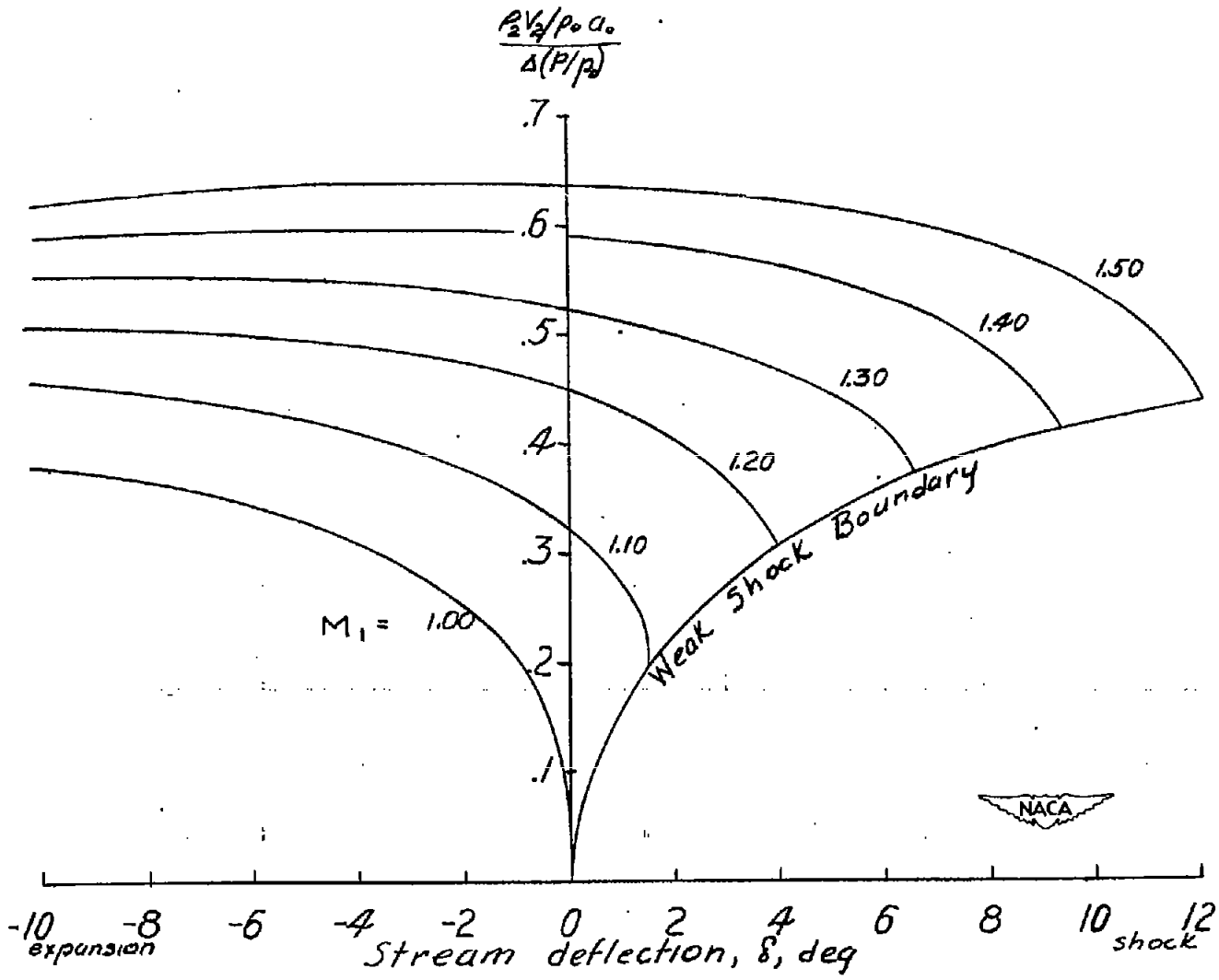

Figure 3.- Effect of stream deflection in the ratio of the change in lateral flow to the static-pressure difference across the disturbance.

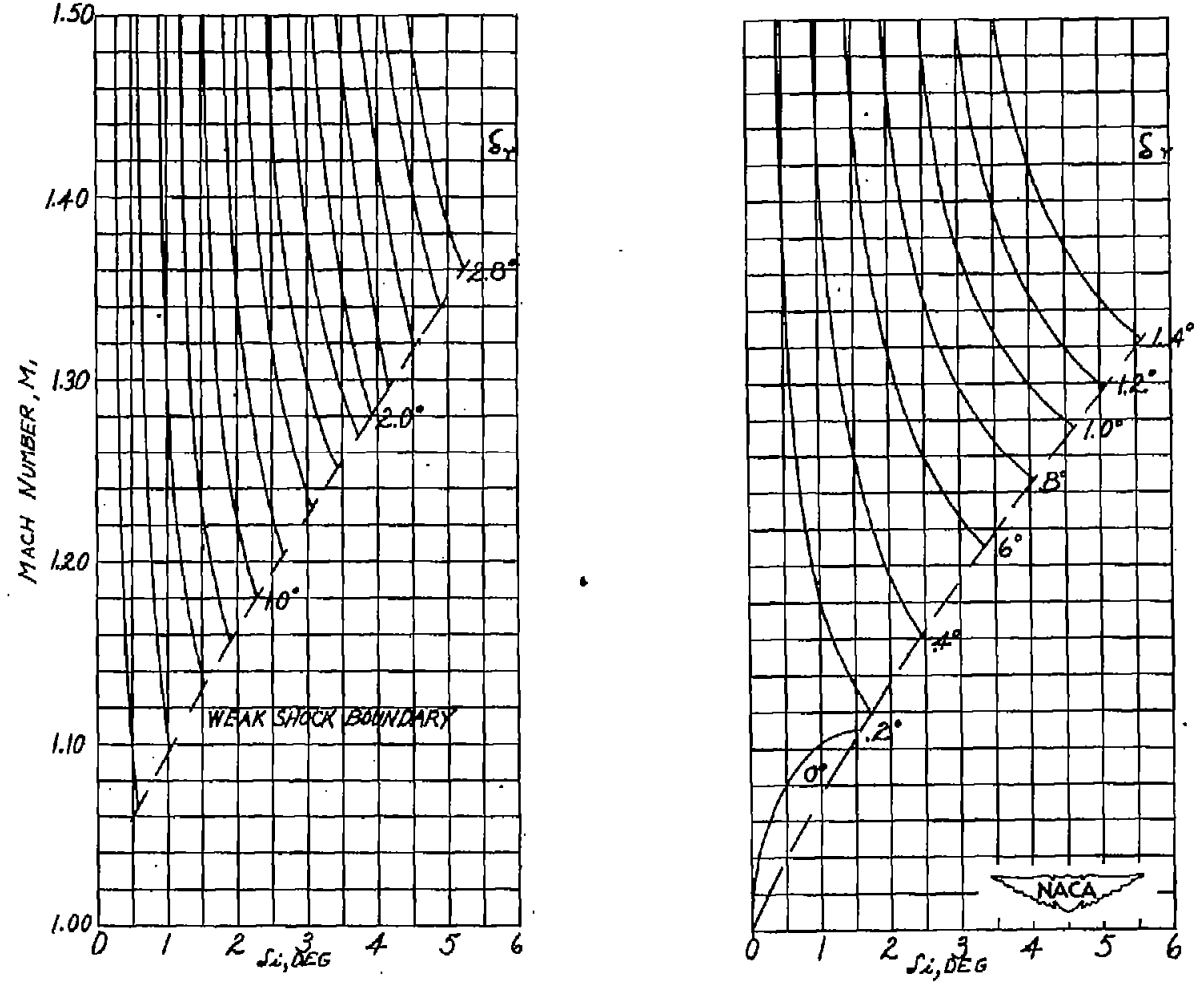

(a) $\frac{g\rho V}{\Delta p} = 0.0055$.

(b) $\frac{g\rho V}{\Delta p} = 0.011$.

Figure 4.- Calculated shock-reflection characteristics of surfaces of constant porosity.

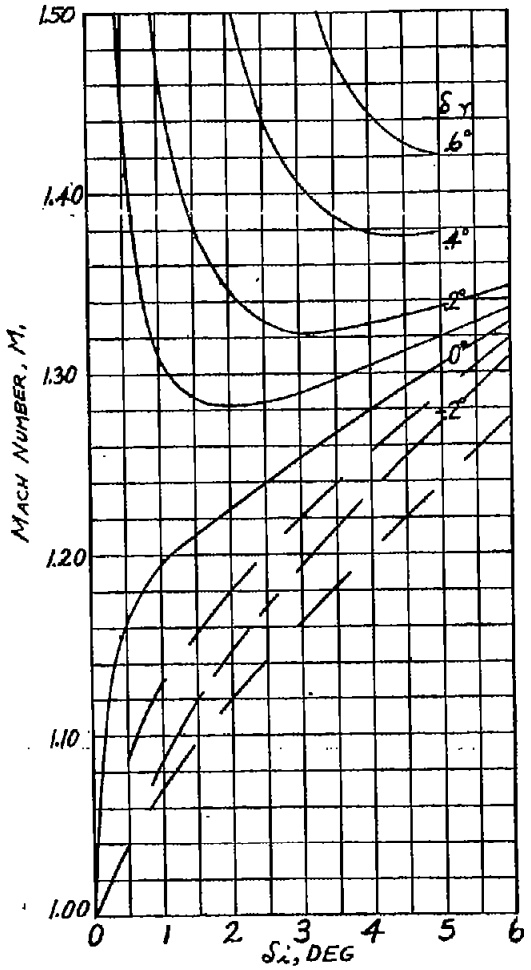

(c) $\frac{g\rho V}{\Delta p} = 0.018$.

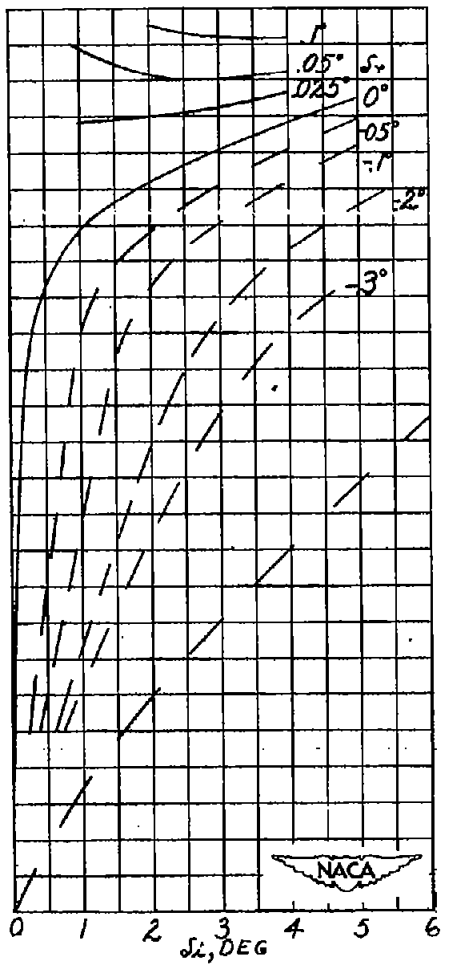

(d) $\frac{g\rho V}{\Delta p} = 0.024$.

Figure 4.- Concluded.

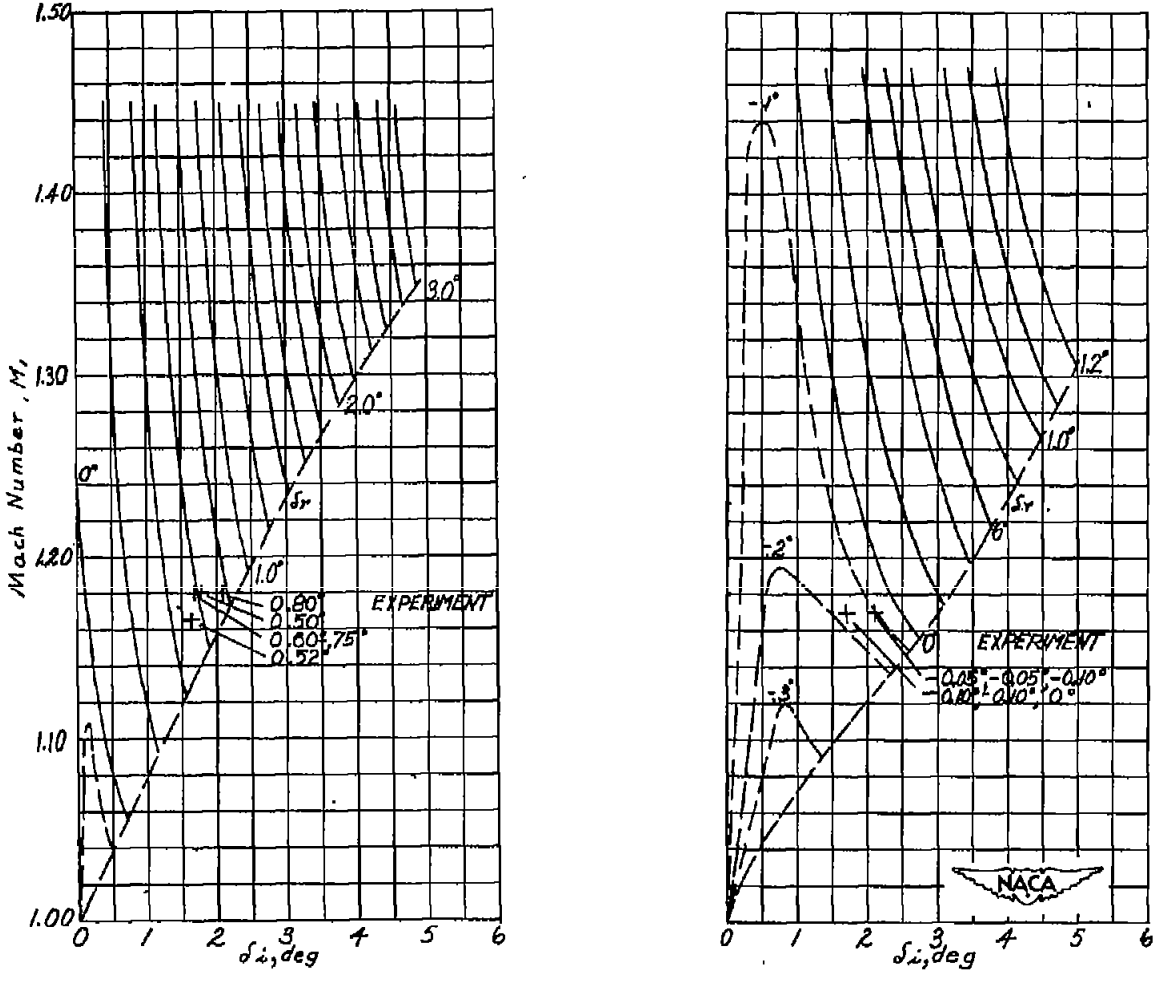

(a) Sintered bronze.

(b) Bonded screen.

Figure 5.- Shock-reflection characteristics of materials of nonlinear-flow-rate variation with pressure drop.

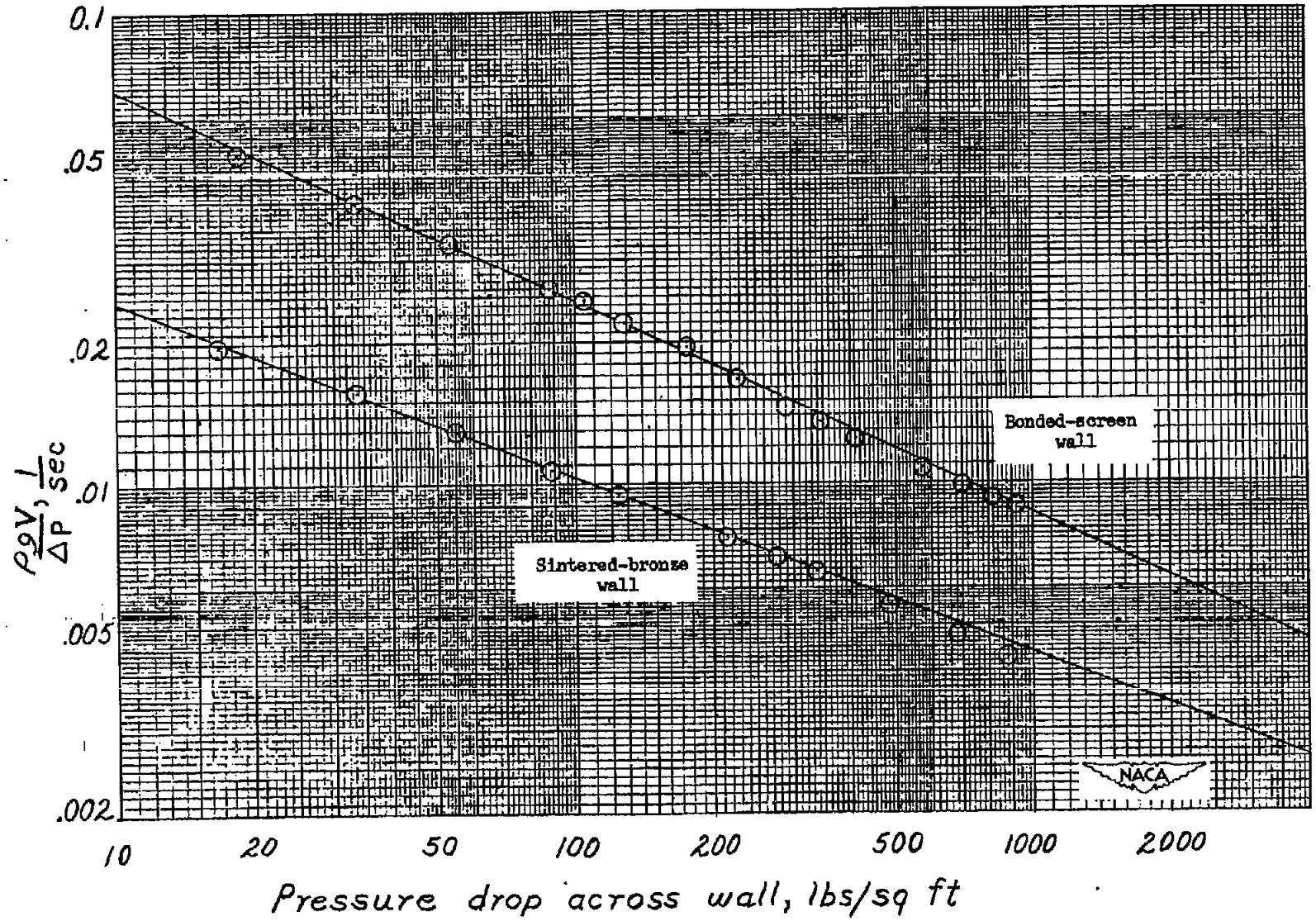

Figure 6.- Porous-wall calibrations.

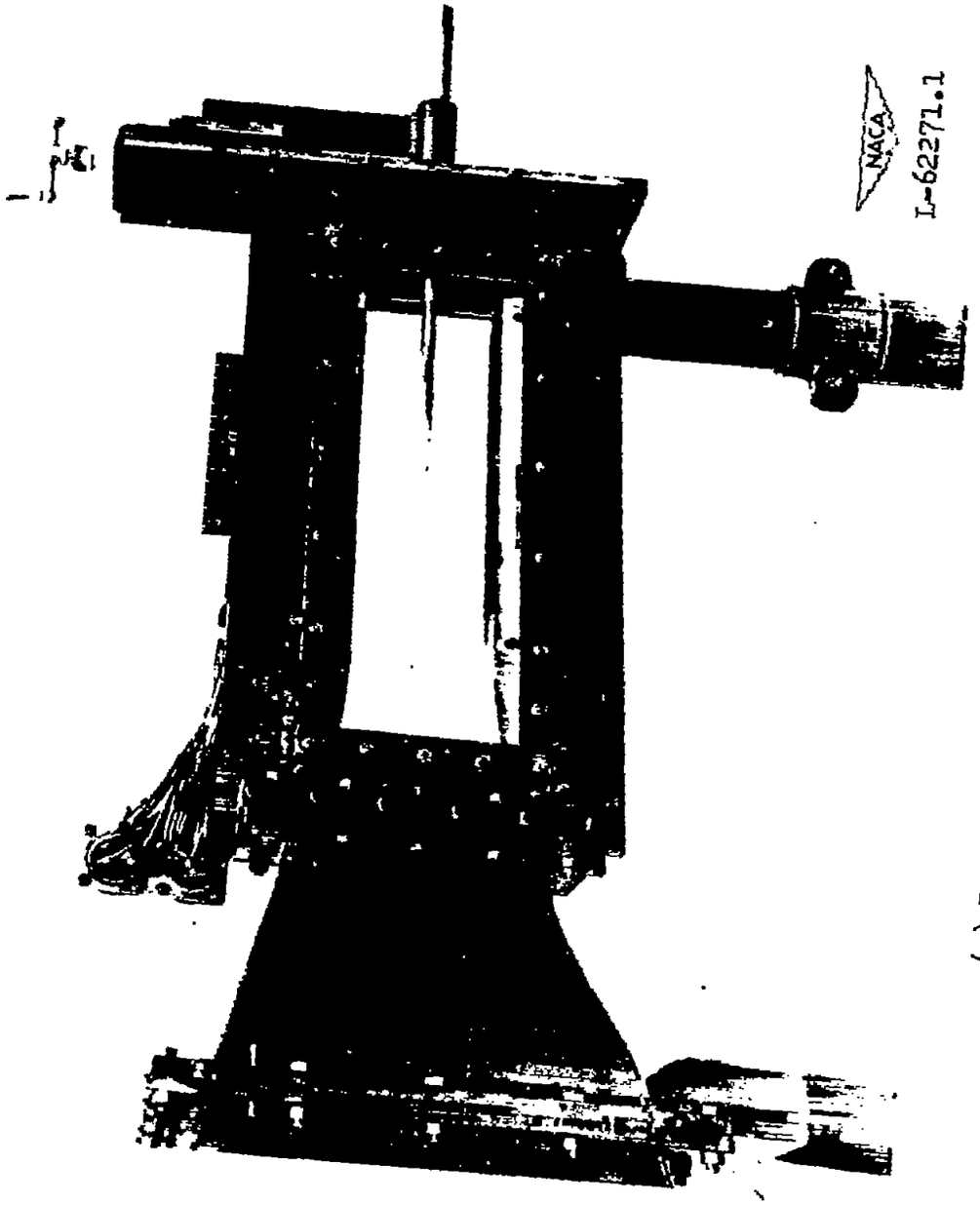

NACA L-62271.1

(a) Porous tunnel with 4° wedge installed.

Figure 7.- Experimental apparatus.

NACA
L-62268

(b) 4° wedge.

Figure 7.- Concluded.

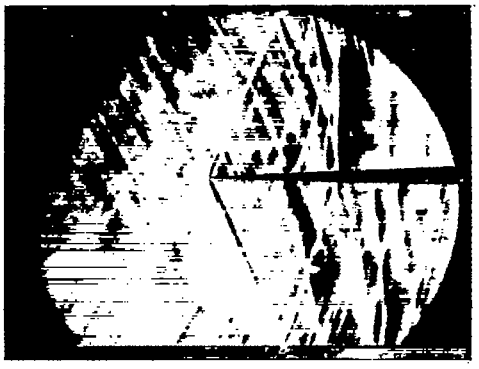

Wall	M_1	δ_i (deg)	M_2	δ_r (deg)
Top	1.18	2.1	1.08	0.8
Bottom	1.18	1.8	1.095	.6

(a) Sintered-bronze walls.

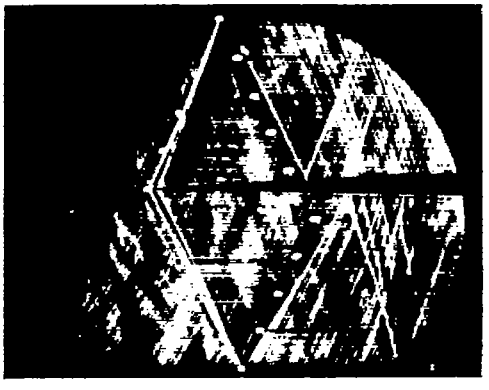

Wall	M_1	δ_i (deg)	M_2	δ_r (deg)
Top	1.17	2.1	1.065	-0.10
Bottom	1.17	1.7	1.09	-.16

(b) Bonded-screen walls.

NACA L-64882

Figure 8.- Schlieren photographs of the flow with the 4° wedge installed in the porous-walled tunnel.

NACA-Langley - 9-13-50 - 275